Journal of Applied Mechanical Engineering
Rastgar and Showkati, J Appl Mech Eng 2017, 6:3
DOI: 10.4172/2168-9873.1000268
Research Article
Open Access

Field Study and Evaluation of Buckling Behaviour of Steel Tanks under Geometric Imperfections

Rastgar M* and Showkati H
Department of Civil Engineering, Urmia University, Iran

Abstract

Shells are among the most frequent structural components which are used in construction and industrial projects. Shell structures are composed of shell bearing elements and mainly used in oil and gas tanks, offshore marine platforms, silos, funnels, cooling towers, ship and aircraft body, etc. Despite the frequent use of steel cylindrical shells, their construction and assembling process has caused main problems. In these structures, there is no possibility for the integrated construction due to their large shell extent and they are built using a number of welded curved panel parts; hence, some geometrical imperfections emerge. Most of these imperfections are caused by the process of welding, transportation, inappropriate rolling, as well as installation and implementation problems. These imperfections have a direct impact on the structural behavior of shells during the buckling and external compressive load. Since in most shell tanks during operation, there is high possibility for the suction (vacuum) state, compressive forces in their thin wall cause buckling and failure. In this research, the imperfections made in steel cylindrical tanks being constructed in one of the refinery site are introduced and evaluated using a field study. Relying on the statistical inference, they are classified and then, by studying the effective factors and origin in their generation, the common imperfections are identified. Later, the impact of common imperfections on the buckling behavior is experimentally evaluated under uniform external pressure. Then, nonlinear numerical analysis of the test specimens is performed. Finally, experimental results, finite element and analytical relations are compared.

Keywords: Field study; Buckling behavior; External pressure; Cylindrical tank; Geometric imperfection

Introduction

Shell structures are the surfaces that separate a volume of space from the rest. From geometrical viewpoint, shell structures have curved initial shapes with the thickness so much less than two other dimensions. In some states of shells, radius-to-thickness ratio reaches 3000. Among the most common methods for strength increase without weight increase is the use of thin-walled shell structures, which have important and beneficial properties owing to their useful structural form and light weight with high strength. The stability type of a structural system depends on parameters such as geometrical properties as well as materials and environmental conditions such as loading conditions. Instability in these structures is theoretically defined as bifurcation point, limit point and dynamic and vibration instability. In Figure 1, axial load-displacement graph of the cylindrical shell is shown [1].

In bifurcation point instability, in which deformations are along the applied loads, member or system is suddenly deformed in the vertical direction. The transfer point from the common deformation mode to deformation variable mode is known as balance bifurcation point. Load at the balance bifurcation point is called critical load. Membrane forces act along the component axis and tangent to the middle surface of the shell plate and the buckling in these structures occurs when the structure converts membrane strain energy into bending strain energy without any change in the applied external load [1]. Several studies about buckling behavior and instability of shells have been done that can be pointed as follows:

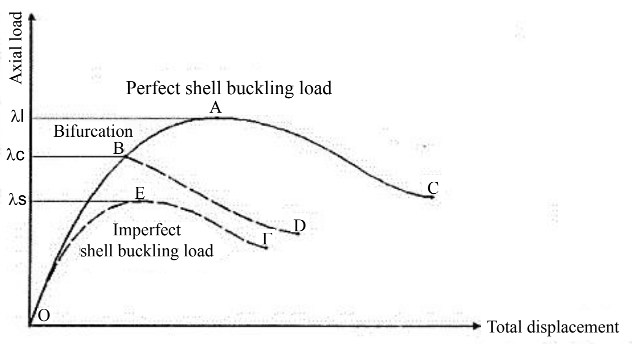

Figure 1: Axial load-displacement graph of the cylindrical shell is shown at limit and bifurcation points.

Influence of primary boundary condition on the buckling of shallow cylindrical Shells was studied by Showkati and Ansourian [2] experimentally. Wang and Koizumi [3] investigated the buckling of cylindrical shells with longitudinal joints under external pressure. Buckling of cylindrical shells with stepwise variable wall thickness under uniform external pressure was considered by Chen, Rotter and Doerich [4]. Aghajari et al. [5] studied buckling of thin cylindrical shells with two-stepwise variable thickness under external pressure experimentally. Experimental and numerical investigation of composite conical shells stability subjected to dynamic loading was investigated by Jalili et al. [6]. Ghazijahani, Jiao and Holloway [7] studied longitudinally stiffened corrugated cylindrical shells under uniform external pressure [8].

Geometric Imperfections and Shell Buckling

In contrast to various structures, the buckling strength of shells with no imperfections is significantly different from the buckling

***Corresponding author:** Rastgar M, Ph.D, Department of Civil Engineering, Urmia University, Iran, Tel: +98 44 3275 2740; E-mail: mrastgar89@gmail.com

Received April 23, 2017; **Accepted** June 02, 2017; **Published** June 06, 2017

Citation: Rastgar M, Showkati H (2017) Field Study and Evaluation of Buckling Behaviour of Steel Tanks under Geometric Imperfections. J Appl Mech Eng 6: 268. doi: 10.4172/2168-9873.1000268

Citation: Rastgar M, Showkati H (2017) Field Study and Evaluation of Buckling Behaviour of Steel Tanks under Geometric Imperfections. J Appl Mech Eng 6: 268. doi: 10.4172/2168-9873.1000268

strength of the same shell with imperfections. This feature puts shells among the structures which are called sensitive to imperfection. In investigating the behavior of shells, effect of imperfections is so important. Imperfections are generally divided into four groups of geometrical imperfections, loading imperfections, imperfections due to boundary conditions, and imperfection associated with physical properties of materials [9-11].

In this classification, geometrical and loading imperfections have a more considerable impact on the bearing capacity of shells, because in the real state, the implemented shells are never complete in geometrical terms and the application of an ideal loading to the shell is not possible in the real state. Geometrical imperfections include all the deviations in the form of structural component compared with its ideal geometrical composition. In the case of shells, geometrical imperfections are determined by deviation from the geometry of the middle surface from the ideal shape. In the construction of shells, due to the large dimensions, curved plates or panels can be used. The seam between various plates of the main source of deviation is in the real form, these deviations or imperfections can be generated as a result of welding or appropriate incompatibility of the plates with larger dimensions than other plates. In some states, geometrical imperfections may strengthen the structure and increase its capacity (Ghazijahani et al [12]. Several studies about imperfection influence on the buckling behavior and instability of shells have been done that can be pointed as follow:

Imperfection influence on the buckling of thin cylindrical shell under uniform external pressure was studied by Lo Frano and Forasassi [8] experimentally. Yang et al. [9] studied buckling of cylindrical shells with general axisymmetric thickness imperfections under external pressure. Fatemi et al. [10] done experiments on imperfect cylindrical shells under uniform external pressure. Inelastic stability of liners of cylindrical conduits with local imperfection under external pressure was studied by Khaled El-Sawy. Ghazijahani et al. [12] has done experiments on dented cylindrical shells under peripheral pressure [13].

Imperfections caused by welding

Steel tanks and silos are considered among the thin-walled structures which are usually constructed by welding a large number of curved panel components to each other. Panels are welded using meridional welding to form vertical paths and attached floors as well as circular and continuous environmental welding for complete shaping of the welding shell wall. The circular and environmental situations

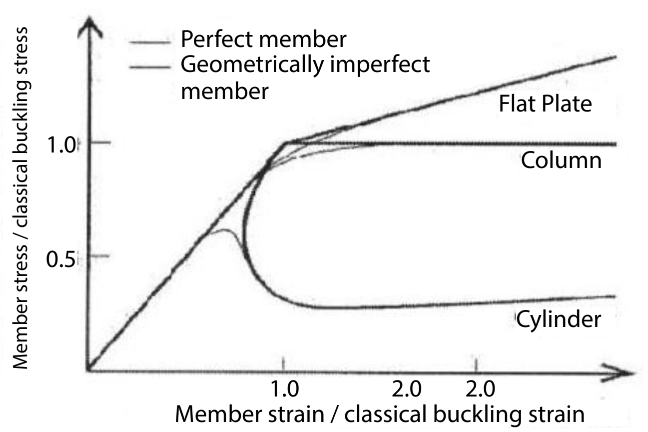

Figure 2: Load-axial displacement graph of bars, plates and shells in perfect and imperfect states.

of meridional welds in a vertical path are usually distanced from the adjacent paths by half of the panel width and, in general, they are attached to each other as patterned welds. Due to the large number of welds, both deformations caused by welding (or troughs and geometrical imperfections caused by welds) and residual stresses have a significant impact on the buckling strength of the shell wall.

In Figure 2, the buckling behavior of bars, plates, and shells is schematically shown. In these curves, the highlighted lines show the system with no geometrical imperfections or perfect, while the dash-line curves represent the corresponding behavior of the imperfect system. As can be observed, the bar and plate elements are not sensitive to imperfection, while domes which are an example of thin-walled structures are very sensitive to imperfections. Figure 2 also shows that secondary balance path (buckling shape) for the bars and plates does not exist in the loading less than the critical load. In some shells under specific loadings, reduction of stiffness after the buckling is so high. Therefore, the buckling shapes in the static balance are left close to loading only via the system change, which can be at the degrees lower than the buckling load [14].

Several studies about weld-induced imperfections influence on the buckling behavior of shells have been done that can be pointed as follow:

Teng, Lin, Rotter and Ding [15] investigated the geometric imperfections in full-scale welded steel silos. In other work, buckling behavior of large steel cylinders with patterned welds was considreed by Hubner, Teng and Saal [16]. Maali et al. [17] investigated the Buckling behavior of conical shells under weld-induced imperfections experimentally.

Analytical Equations for Buckling of Cylindrical Shells

Stability equation of cylindrical shells has been derived as follows:

$$D\nabla^8 + \frac{Et}{R^2}W,xxxx + \frac{1}{R}q\nabla^4 w,\theta\theta = 0 \tag{1}$$

The general solution of this equation is as follows:

$$w = \left(c_1 \sin\lambda x + c_2 \cos\lambda x + c_3 x + c_4\right)\sin n\theta \tag{2}$$

In which m and n are $\lambda = \frac{mx}{L}$, m, n = 1,2, 3,…

Using the boundary conditions, c1 to c4 constants are obtained. Considering simple end conditions for the ends of the cylindrical shell as well as m = 1, uniform external pressure buckling load is calculated as follows [13]:

$$p_{cr} = E\frac{t}{R}\left\{\frac{\left[\left(\frac{\pi R}{L}\right)^2 + n^2\right]^2}{n^2}\frac{\left(\frac{t}{R}\right)^2}{12\left(1-\nu^2\right)} + \frac{\left(\frac{\pi R}{L}\right)^4}{n^2\left[\left(\frac{\pi R}{L}\right)^2 + n^2\right]^2}\right\} \tag{3}$$

The number of circumferential waves of cylindrical shell formed in the body of the tank is as follows [2]:

$$n = \sqrt[4]{\frac{6\pi^{2\sqrt{1-\nu^2}}}{\left(\frac{L}{R}\right)^2\left(\frac{t}{R}\right)}} \# 2.74\sqrt{\frac{R}{L}}\sqrt{\frac{R}{t}} \tag{4}$$

Considering the application of uniform external pressure to the roof of cylindrical tanks causes a uniform axial force to the body of tanks, and the buckling load of these tanks under the simultaneous

Citation: Rastgar M, Showkati H (2017) Field Study and Evaluation of Buckling Behaviour of Steel Tanks under Geometric Imperfections. J Appl Mech Eng 6: 268. doi: 10.4172/2168-9873.1000268

Figure 3: Circumferential sheets installation process in the body of tank and generation of different imperfections.

Figure 4: Types of observed imperfections in the field study of tanks.

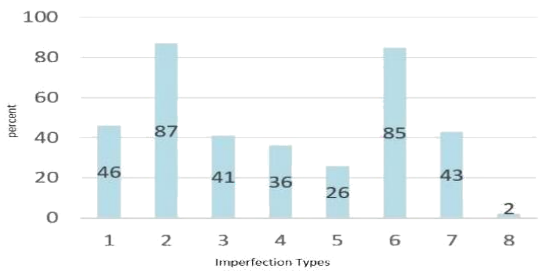

Figure 5: Frequency distribution graph of the imperfection types in all tanks.

effect of uniform lateral pressure and axial load is obtained by the following equation:

$$P_{cr} = \frac{1}{R}\frac{\left(\bar{m}^2+n^2\right)^4\left(\dfrac{D}{R^2}\right)+\bar{m}^4\left(1-v^2\right)C}{\left(\bar{m}^2+n^2\right)^2\left(n^2+0.5\bar{m}^2\right)} \quad (5)$$

In which t, R and L are thickness, radius and length of cylindrical shell respectively. By using the approximate equation, the buckling load caused by uniform external pressure along with axial load is obtained equal to 23.4 kPa and also the number of circumferential waves formed in the body of the tank is 13 waves based on Equation n. In this study, the amount of the obtained buckling load is used for the evaluation and comparison of the results taken from finite element analysis and laboratory samples.

Field Survey

In order to store oil products in a refinery site, the construction of numerous tanks has begun, which are being implemented as steel cylindrical tanks in 2 different sizes:

1. **Large storage tanks:** The first type of tanks has the height of 12 m, diameter of 23 m, and sheet thickness of 18 mm and 3 of them are under construction.

2. **Small storage tanks:** The second type of tanks has the height of 7.5 m, diameter of 13.5 m, and sheet thickness of 14 mm and 5 of them are under construction.

For the construction of these tanks, the steel sheets with the dimensions of 6 × 1.5 m and thickness of 18 mm and 14 mm are used. These sheets are manufactured by Mobarakeh Steel Company and directly sent to the site. The sheets are entered into the rolling device and the curvature operations are performed during several steps to reach the radius of the tank. Then, they are transferred to the relevant location by the special vehicles for transporting the rolled sheets and their installation operations are carried out using the crane and human force. From this step on, numerous imperfections caused by various implementation factors are made; some of them are partly modified and some others are remained in the tank even after the implementation is complete. The steps are shown in Figure 3.

According to this figure, the rolled sheets are put in their place by the crane and then temporarily welded next to each other (tack weld). When the first layer is completed, the next layers are implemented similar to the first layer. The rolling, transportation, and installation of these sheets cause various imperfections in the implemented layer. As shown in Figure 3, the edges of the environmental sheets do not match each other; these edges should get close to each other by a chain and a crane until the imperfection is modified. Basically, some of the created imperfections are removed from the body of the tanks and some others are left permanently.

In this research, after attending the tank implementation location and field monitoring of the installation of circumferential sheets, various type of imperfections is observed, which are classified as follows:

1-Imperfection I: Non-compliance to the edges of the consecutive horizontal rows that occurred outside and inside.

2- Imperfection II: Vertical seam isn't executed properly and is sharp towards inside or outside.

3- Imperfection III: Vertical edges aren't parallel.

4- Imperfection IV: Horizontal edges aren't aligned.

5- Imperfection V: Caused by unsuitable rolling

6- Imperfection VI: Different layers in height aren't vertical.

7- Imperfection VII: Effect of welding temperature which usually appears in the form of circumferential

8- Imperfection VIII: Wind effects causing troughs or bulge, in the peripheral of lastest layer of tank.

These imperfections are shown in Figure 4.

By continuing the field study on the implementation of these tanks in a 5-month period and statistical inference from the imperfections introduced in all the tanks being constructed in the refinery site, the frequency distribution graph of the imperfections is drawn, as shown in Figure 5.

In this figure, the horizontal axis shows the type of imperfection and the vertical axis is the frequency percentage of the corresponding imperfection. Accordingly, it can be seen that, from among all the introduced imperfections, imperfection types 2 and 6 occur more frequently than others, respectively. It should be noted that this statistic is periodic and the number may change until the end of tank body implementation and roof installation.

Experimental Program

For the experimental evaluation of the impact of imperfections on the buckling behavior of tanks, two experimental specimens made with the scale of 1/20 of the real tank are made with the following characteristics: The first specimen has the diameter of 115 cm, height of 60 cm, conical roof with the height of 20 cm, tank body plate thickness of 1 mm, and floor and roof thickness of 1.5 mm in an integrated form. The second specimen is panelized; each panel which has the dimensions of 30 × 7.5 cm and tank height of 60 cm is composed of 8 layers in height, tank diameter of 115 cm, as well as 12 panels in the environment; in total, it has 96 panels, a conical roof with the height of 20 cm, tank body plate thickness of 1 mm, and floor and roof thickness of 1.5 mm.

In order to prevent the floor and roof buckling of these tanks influenced by external pressure, strengthening straps with the section of 2 × 0.5 cm are used. These straps could increase the bending stiffness in the roof and floor of the tanks; so, under the uniform external pressure, these two parts maintain their initial situation and do not buckle as a result, only the body of the tanks starts to move and buckles. Despite high accuracy in producing the laboratory specimens, various imperfections emerge in these specimens, the major one of which includes imperfections caused by welding due to low thickness of sheets used as troughs in the body, troughs in the floor and roof of the specimens caused by transportation from the workshop to laboratory, as well as movement at different places in the laboratory. The specimens are shown in Figures 6 and 7.

Figure 6: Experimental specimen tank1 in an integrated form.

Figure 7: Experimental specimen tank 2 in panelized form.

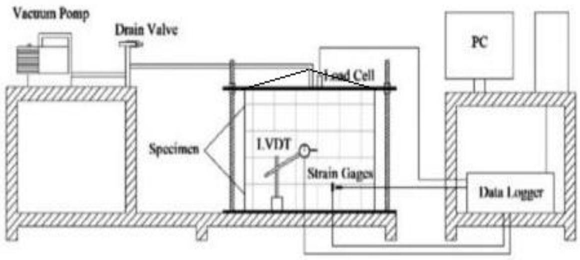

Figure 8: Schematic view of laboratory equipments and experimental specimen.

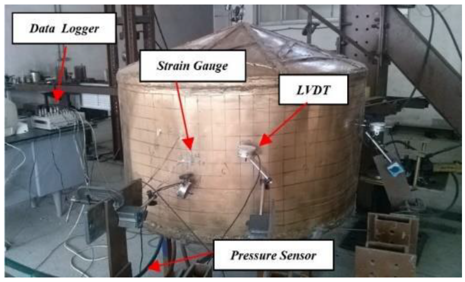

Figure 9: Installation of measurement devices on the experimental specimen.

Testing of Specimens and Evaluation of Results

Uniform external pressure loading

In order to evaluate the buckling behavior in the experimental specimens influenced by uniform external pressure, the suction device is used. It is an electro-pump device that discharges the air inside the tank with the constant flow of 40 m^3/h to the outside. So, by discharging the air inside the tank, the atmospheric pressure is uniformly imported into the external surfaces of this tank and loading is applied as uniform external pressure to the tank. Since air discharge flow of the tank is too high, it is necessary to embed a control valve to adjust the discharge flow and thus control the external pressure.

In order to measure the internal pressure in the tank, a pressure gauge is used. This device shows the moment-to-moment pressure inside the tank, which is decreased due to the discharge by the suction device. So, the external pressure is obtained by subtracting atmospheric pressure and the pressure inside the tank. There are three holes in the tank floor: the first hole is connected to the suction device, through which discharge operation is done (applying uniform external pressure). The second hole is connected to the discharge valve and controls the flow of tank discharge (loading control) and the third one is connected to the pressure gauge to measure the internal pressure (loading measurement). In Figure 8, the laboratory equipment, including the suction pump for loading application, loading control valve, loading measurement device, deformation measurement devices, location of test samples, the data logger, and the computer are schematically shown.

Test procedure and measurement devices

In order to take the experimental specimens deformation, measurement devices are installed in different parts of these specimens in the middle of the height radially and also at the top of the conical roof of the specimens. These devices include LVDT, strain gauge and pressure sensor. LVDTs take the directional displacements vertically, horizontally, or radially in the location they are installed and send

Citation: Rastgar M, Showkati H (2017) Field Study and Evaluation of Buckling Behaviour of Steel Tanks under Geometric Imperfections. J Appl Mech Eng 6: 268. doi: 10.4172/2168-9873.1000268

them to the data logger. The strain gauges are the electronic circuits that are attached using a special adhesive in the desired location and measure strain in their installed direction and send it to the computer. In this research, in all the tests, five LVDTs and two horizontal and vertical strain gauges are used to record the deformation of different parts of the experimental specimens. In Figure 9, a sample of these measurement devices which is installed on the experimental specimens is represented.

Test implementing

Air discharge from tank 1 starts by turning on the suction pump device and the difference between the internal and external pressure of the tank is gradually increased. As a result, external pressure is gradually applied to the tank and the initial buckling of the tank body begins. By increasing the external pressure, the number of the waves formed in the tank body is also increased and the tank moves toward full buckling. Then, after making 12 waves in the tank, the buckling of the body becomes complete and, finally, at the external pressure of 21.6 kPa, the tank trough suddenly happens and the tank becomes instable. Figure 10 shows full buckling and Figure 11 demonstrates instability and failure of the experimental tank 1.

In the specimen test 2, similar to specimen 1, loading continues

Figure 10: Full buckling of specimen 1 and instability threshold.

Figure 11: Failure of the experimental tank no.2.

Figure 12: The sudden Instability of the specimen no.2.

Figure 13: Weld line failure of the specimen no.2.

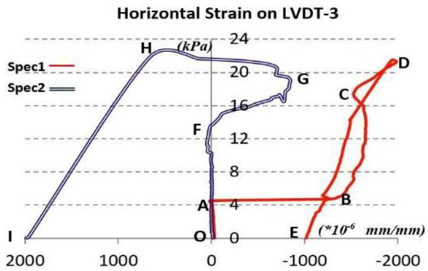

Figure 14: Horizontal strain diagram of tanks 1 and 2 at the location of LVDT3 in terms of external pressure.

gradually and in a controlled manner to the trough stage and full instability. In this sample, in contrast to the previous sample, the environmental waves are formed irregularly and randomly at different points of the tank body. Finally, without completing the environmental waves and getting the tank to the full buckling state, one of the environmental panels becomes instable at the external pressure of 21.84 kPa due to the vertical weld line failure. In Figures 12 and 13, the instability and weld line failure of the experimental tank 2 are shown.

According to these figures, the instable form of specimen 2 is completely different from that of specimen 1 and no regular circumferential waves can be seen in the tank body as sample 1. In other words, full buckling in the tank body 2 is not observed; but, due to the weakness of the vertical weld line in one of the panels, local buckling occurs, which makes the whole tank instable. If the weld line did not fail, a higher buckling load than sample 1 was expected to be obtained. However, in the current state, the buckling load caused by the external pressure of this sample shows a higher value than sample 1. The reason is the existence of welded lines in the panels composing the tank body, which increases the membrane strength of the tank against the compressive loads, similar to the circumferential stiffeners.

Evaluation of experimental results

By taking the data obtained from the measurement devices installed at different parts of these tanks, strain and radial displacement graphs of these points are drawn relative to the applied external pressure. Figure 14 shows the horizontal strain diagram in terms of external pressure at the half of the body height of tanks 1 and 2 at LVDT3, which is almost located in the vicinity of the instability of these tanks. Horizontal strains show the environmental deformations of the tank.

Specimen 1 at point A bears 5 kPa load and has considerable strain changes. The tank body 1 locally buckles at this point and a leap can be seen on the graph from A to B, while specimen 2 has no strain changes

Citation: Rastgar M, Showkati H (2017) Field Study and Evaluation of Buckling Behaviour of Steel Tanks under Geometric Imperfections. J Appl Mech Eng 6: 268. doi: 10.4172/2168-9873.1000268

at these points and is almost without any strain to the load of 14 kPa or point E. This issue shows better initial strength of tank 2 than tank 1. Specimen 1 represents no great strain changes from points B to C. Finally, it becomes instable at point D and, then, from points D to E, it is located in the unloading state.

When the unloading is finished, the permanent strains are left in the tank body 1 (point E). In tank 2, from points F to G, considerable strain changes can be observed. At point G, the direction of the strains is changed by continuing the loading and the tank body moves to the opposite side to reach point H and become instable. Then, the specimen is located in the unloading state to get the pressure inside tank 2 to the atmospheric pressure. In this tank, permanent strains are left (point I), but their value is almost twice as much as that of tank 1.

Figure 15 shows the radial displacement of the body of tanks 1 and 2 at the location of LVDT3 in terms of external pressure. This point is almost close to the buckling and instability site of tanks 1 and 2. Tank 1 shows no significant radial displacement from the start of loading to point A.

From points A to B, a leap can be seen in the graph that is related to the local buckling of LVDT3 site. From points B to C, with an increase in the external pressure, the radial displacement is also increased and reaches 12 mm at point C. Then, the tank suddenly becomes instable and the unloading step is started. But, radial displacement is also increased to reach 20 mm at point E. Afterwards, due to the instability at the adjacent points, the radial displacement is decreased until the external pressure reaches 0 at point F and the radial displacement of 4 mm is remained in tank No.1.

In tank No.2, with the start of the external pressure, less radial displacement can be observed compared with tank 1 until becoming 5 mm at point H. Then, direction of the radial displacement is changed and displacement continues in the opposite direction with the loading continuation until instability and trough of tank 2 occur at point G suddenly as a result of the weld line failure in one of the panels. From this step on, unloading is started and finished at point K.

By comparing these graphs, it can be seen that the LVDT3 displacement from tank 1 at the instable moment is maximum 13 mm and then, during the unloading, it is about 20 mm at point D. For tank 2, it is maximum 5 mm at point H. LVDT3 is almost close to the instability location in both tanks. It is obvious that the membrane strength in tank 2 is more than that of tank 1 at the moment of buckling and trough, because the welding lines of the panels composing the body of tank 2 increase the membrane strength similar to circular stiffeners.

In this research, vertical displacement in the conical roof of the samples is also considered, which is shown in Figure 16 in terms of the applied external pressure. The data in these graphs are obtained from LVDT7 for tank 1 and LVDT8 for tank 2. By studying these graphs, it can be seen that, with the start of loading, the roof displacement is also started for both tanks, but it shows a larger value in tank 1 than tank 2 so that the maximum roof displacement for tanks 1 and 2 is almost 11 mm (point A) and 26 mm (point B) which is approximately 2.5 times, respectively.

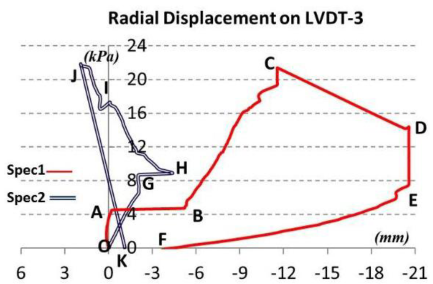

Figure 15: Radial displacement of the body of tanks 1 and 2 at the location of LVDT3 in terms of external pressure.

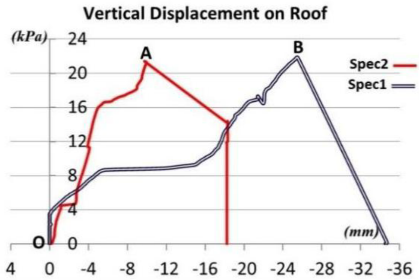

Figure 16: Vertical displacement in the conical roof of the specimens 1 and 2 in terms of external pressure.

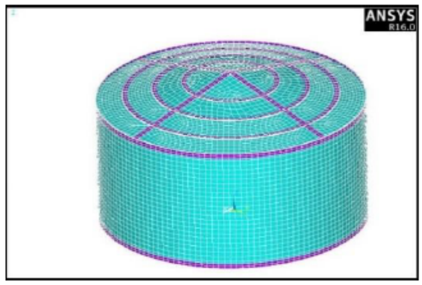

Figure 17: FEM model of tank no.1 in ANSYS.

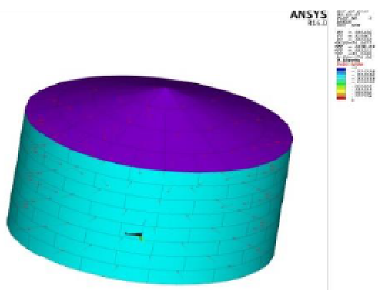

Figure 18: FEM model and loading of tank no.2 in ANSYS.

Finite Element Analysis of the Specimens

In order to evaluate the buckling behavior of the test specimens, numerical modeling of the specimens is carried out by the finite element software. Modeling of tank 1 is performed as a continuous sheet and tank 2 is panelized with the sheet thickness of 1 mm in the environment and thickness of 1.5 mm in the floor and roof. Similar to the experimental specimens, in order to prevent the buckling of the roof and floor, stiffeners quite similar to the specimens made in the laboratory are used. In Figures 17 and 18, finite element model and loading of tanks 1 and 2 are demonstrated.

In this study, the nonlinear analysis of buckling including geometric nonlinearity and material nonlinearity is carried out for the finite element models of tanks 1 and 2. By drawing the load-displacement diagram at various points such as LVDT3 location, which is the location of trough and instability of the laboratory specimens, the approximate value for the external pressure leading to the buckling of tanks 1 and 2 is determined.

In Figure 19, the full buckling of the modeled tank 1 is shown before instability in the nonlinear state. As can be seen, 12 full waves are created in the environment of the tank body. In the experimental state, after full buckling and before the instability of tank 1, 12 waves are formed in the body of the tank, so a good correspondence can be observed.

Figure 20 shows the load-displacement graph of the finite element models for tanks 1 and 2. In specimen 1, with the start of loading, small deformations start in the body of the tanks to point a. Then, by increasing the external pressure, radial deformations of the tank body 1 significantly increase to reach 11 mm at point b. The oscillations in the graph of tank 1 in the b-c region show the formation of the environmental waves around the studied point. At point c, the buckling of the tank body is completed at the pressure of 23 kPa and 12 full waves are created. Afterwards, by increasing the loading, the modeled specimen of tank 1 enters the post-buckling step and continues until the pressure of 30 kPa, while the post-buckling step is not seen in the experimental specimen and the specimen becomes instable after point c. Therefore, point a show the start of the buckling of specimen 1 at the load of 16 kPa, point b shows the full buckling of the starting point at the load of 21 kPa, the range bc demonstrates the buckling of other points, point c shows the full buckling at the pressure of 22 kPa, cd is the buckling step of the specimen to the pressure of 30 kPa, and the load of point c indicates the failure of the experimental specimen.

It can be seen that start of the buckling for specimen 1 is 31.9%

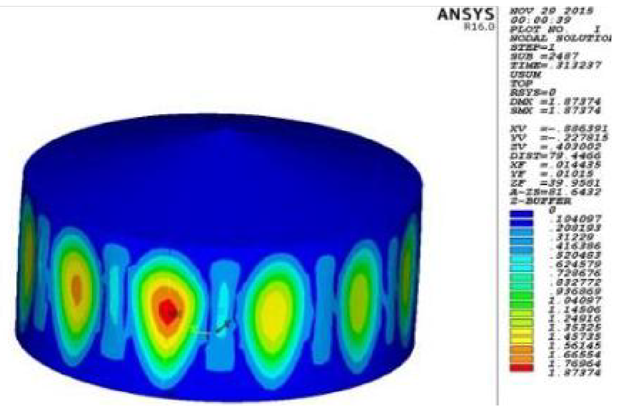

Figure 19: Full buckling of the modeled tank 1 in the non-linear state.

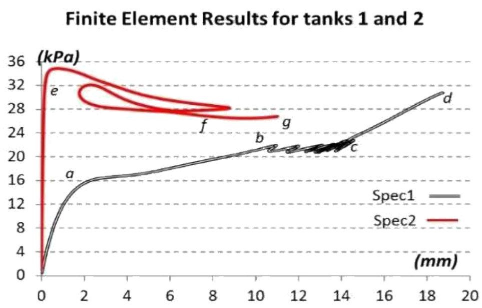

Figure 20: Load-deformation graph of the FEM models for tanks 1 and 2.

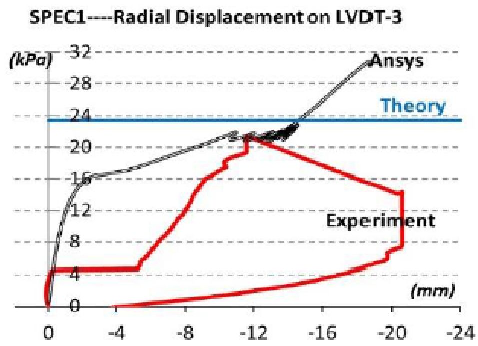

Figure 21: Compartion of obtained results for specimen 1.

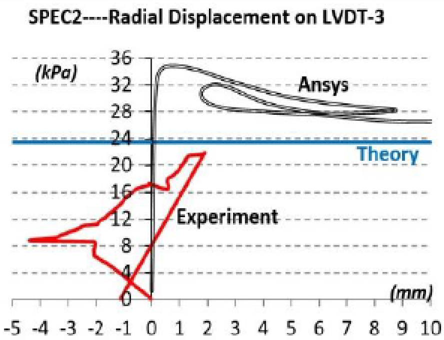

Figure 22: Compartion of obtained results for specimen 2.

less than the approximate value, its full buckling is 6.4% less than the approximate load, and the post-buckling load is 27.6% higher than the approximate load and 38.9% higher than the buckling load leading to failure.

In the finite element specimen of tank No.2, no radial displacement can be seen by the start of the loading to point e (almost 1 mm). With continuing the loading, the local buckling starts at point f and the amount of radial displacement of specimen 2 in this step reaches 8 mm. Due to the local buckling adjacent to the studied point, the return can be seen in the curve of tank 2. By continuing the loading, the displacements continue to 11 mm at point g and, then, the finite element model becomes unstable. The amount of external pressure at the instability moment is almost 28 kPa.

Summary of the obtained results from the experiment, finite element, and approximate equation is shown in Figures 21 and 22 for tanks 1 and 2, respectively.

According to the figures, it can be observed that the buckling load of non-linear finite element of tanks 1 and 2 is 23 kPa and 28 kPa, respectively. However, the buckling load leading to instability in tanks 1 and 2 obtained from the experiment models is 21.6 kPa and 21.8 kPa, respectively, and the buckling load of these tanks is 23.5 kPa according to the approximate equation (5).

Conclusions

With the field study of the implementing tanks in one of the refinery site, various imperfections are observed in these tanks and classified into 8 categories. The origin of the imperfections is different factors such as human resources, inappropriate rolling, welding, lack of appropriate implementation tools, transportation, arrangement, crane opperation, natural factors like wind, and poor implementation by inexperienced people.

1. By investigating the imperfections on the data, it is clear that imperfection types 2 and 6 are more frequent than others.

2. Membrane resistance of tank 2 in initial buckling and failure, is more than that of tank 1 because the existence of the welding lines of the panels forming the tank body 2, which increases the membrane resistance like circular stiffeners.

3. By comparing FEM, experimental and theory results of specimen 1 it was observed that the nonlinear analysis is 6.5% more than the experimental case and 2.1% less than the theory. The experimental case is also 8% less than the approximate equation.

4. By comparing FEM, experimental and theory results of specimen 2 it was observed that the nonlinear analysis is 28.5% higher than the experimental case and 19% higher than the theory. The experimental case is also 7.2% less than the approximate equation.

Non-linear analysis of specimen 1 demonstrates that the start of buckling in this specimen is 31.9% less than the approximate value, the full buckling is 6.4% less than the approximate value, and the post-buckling load is 27.6% higher than the approximate value and 38.9% higher than the buckling load leading to the trough.

References

1. Farshad M (1983) Stability of structures. (2nd edn), Mc Graw Hill, New York.
2. Showkati H, Ansourian H (1995) Influence of primary boundary condition on the buckling of shallow cylindrical shells. Constructional Steel Research 36: 53-75.
3. Wang JH, Koizumi A (2010) Buckling of cylindrical shells with longitudinal joints under external pressure. J Thin-Walled Structures 48: 897-904.
4. Chen L, Rotter JM, Doerich C (2011) Buckling of cylindrical shells with stepwise variable wall thickness under uniform external pressure. J Engineering Structures 33: 3570-3578.
5. Aghajari S, Showkati H, Abedi K (2011) Experimental investigation on the buckling of thin cylindrical shells with two-stepwise variable thickness under external pressure. Int J of Struct Eng Mech 39: 849-860.
6. Jalili S, Zamani J, Shariyat M, Jalili N, Ajdari MAB, et al, (2014) Experimental and numerical investigation of composite conical shells' stability subjected to dynamic loading. J Structural Eng Mech 49: 555-568.
7. Ghazijahani TG, Jiao H, Holloway D (2015) Longitudinally stiffened corrugated cylindrical shells under uniform external pressure. J Construct Steel Res 110: 191-199.
8. Lo-Frano R, Forasassi G (2009) Experimental evidence of imperfection influence on the buckling of thin cylindrical shell under uniform external pressure. J Nuclear Eng and Des 239: 193- 200.
9. Yang L, Chen Z, Chen F, Guo W, Cao G (2013) Buckling of cylindrical shells with general axisymmetric thickness imperfections under external pressure. European J Mechanics A/Solids 38:90-99.
10. Fatemi SM, Showkati H, Maali M (2013) Experiments on imperfect cylindrical shells under uniform external pressure. J Thin-walled Structures 65:14-25.
11. Khaled El-Sawy M (2013) Inelastic stability of liners of cylindrical conduits with local imperfection under external pressure. J Tunnelling and Underground Space Technology 33: 98-110.
12. Ghazijahani TG, Jiao H, Holloway D (2014) Experiments on dented cylindrical shells under peripheral pressure. J Thin-Walled Structures 84: 14-25.
13. Brush DO, Almorth BO (1975) Backling of bears, plates and shells. Mc Graw Hill, New York.
14. Vinson JR (1998) The behavior of thin-walled structures: Beams, plates and shells. Kluwer Academic Publisher, Mechanics of Surface Structures 8.
15. Teng JG, Lin X, Rotter JM, Ding XL (2005) Analysis of geometric imperfections in full-scale welded steel silos. J Engineering Structures 27: 938-950.
16. Hubner A, Teng JG, Saal H (2006) Buckling behavior of large steel cylinders with patterned welds. Int J Presure Vessels and Piping 83: 13-26.
17. Maali M, Showkati H, Fatemi SM (2012) Investigation of the buckling behaviour of conical shells under weld-induced imperfections. J Thin-walled Structures 57: 13-24.